

An empirical approach to estimating hydrocarbon column heights for improved pre-drill volume prediction in hydrocarbon exploration

Edmundson, I.¹, Davies, R.², Frette, L.U.³, Mackie, S.², Kavli, E.A.⁴, Rotevatn, A.¹, Yielding, G.⁵, Dunbar, A.²

¹ Department of Earth Science, University of Bergen, Allégaten 41, 5007 Bergen, Norway

² DEA Norge AS, Jåttåflaten 27, 4007 Stavanger, Norway

³ Capricorn Energy, Jåttåvågveien 7, 4020 Stavanger, Norway

⁴ IFP School, 232 Avenue Napoléon Bonaparte, 92852 Rueil-Malmaison, France

⁵ Badley Geoscience Ltd, North Beck House, North Beck Lane, Hundleyby, Spilsby Lincolnshire, PE23 5NB, UK

isabel.edmundson@uib.no, roy.davies@wintershaldea.com,
lars.ulsund.frette@gmail.com, sean.mackie@wintershaldea.com,
emilieak@online.no, atle.rotevatn@uib.no, graham@badleys.co.uk,
alex.b.dunbar@gmail.com

This manuscript is a preprint and will be submitted to **AAPG Bulletin**. This manuscript has not undergone peer-review. Subsequent versions of this manuscript may have different content. If accepted, the final version of this manuscript will be available via the '*Peer-reviewed Publication DOI*' link on the right-hand side of this webpage. Please feel free to contact Isabel directly or to comment on the manuscript using **hypothes.is** (<https://web.hypothes.is/>). We welcome feedback!

1 An empirical approach to estimating hydrocarbon column heights for improved
2 pre-drill volume prediction in hydrocarbon exploration

3

4 Edmundson, I.¹, Davies, R.², Frette, L.U.³, Mackie, S.², Kavli, E.A.⁴, Rotevatn, A.¹,
5 Yielding, G.⁵, Dunbar, A.²

6 ¹ Department of Earth Science, University of Bergen, Allégaten 41, 5007 Bergen,
7 Norway

8 ² DEA Norge AS, Jåttåflaten 27, 4007 Stavanger, Norway

9 ³ Capricorn Energy, Jåttåvågveien 7, 4020 Stavanger, Norway

10 ⁴ IFP School, 232 Avenue Napoléon Bonaparte, 92852 Rueil-Malmaison, France

11 ⁵ Badley Geoscience Ltd, North Beck House, North Beck Lane, Hundleby, Spilsby
12 Lincolnshire, PE23 5NB, UK

13

14 isabel.edmundson@uib.no, roy.davies@wintershalldea.com,

15 lars.ulsund.frette@gmail.com, sean.mackie@wintershalldea.com,

16 emilieak@online.no, atle.rotevatn@uib.no, graham@badleys.co.uk,

17 alex.b.dunbar@gmail.com

18

19 **Acknowledgements**

20 We wish to thank DEA Norge AS for fully funding the PhD project related to this

21 publication and for providing access to their regional seismic and well databases. In

22 addition, we wish to thank Bernhardt Ujetz, Markus Mohr, Matthias Riede, Olaf

23 Kuchel and Bastian Wirth at DEA AG and Graeme Keith from Decision Risk Analytics

24 for inspirational discussions on the empirical dataset and the forward probability

25 approach used in this study. Schlumberger are acknowledged for providing academic
26 Petrel® licenses to the University of Bergen for seismic interpretation, as are ESRI
27 for provision of ArcMap® licenses used to produce maps for this publication.

28 **Abstract**

29 Estimating pre-drill volumes in hydrocarbon exploration involves dealing with
30 geological and technical uncertainties. The prediction of the hydrocarbon column
31 height is widely recognized as the primary driver of uncertainty in volumetric
32 estimates. The oil and gas industry continues to renew efforts to limit such
33 uncertainties because of the potential economic costs of inaccurate estimation, yet
34 estimation of pre-drill volumes remains an in-exact science. This study introduces
35 new empirical data from the Norwegian Continental Shelf, and aims to improve
36 accuracy in hydrocarbon column height prediction. We use column height, trap height
37 and burial depth data to calculate the degree of hydrocarbon trap fill for each of the
38 242 studied discovery wells. The data is aggregated into a simple forward probability
39 model to calculate the probability of encountering different ranges of trap-fill, based
40 on burial depth and trap height. The distribution of trap-fill ratios clearly correlates
41 with both trap height and burial depth, thus indicating that the same pre-drill column
42 height distribution should not be used for all prospects. These findings strongly
43 suggest that the prospect's dimensions and burial depth are used alongside other
44 technical subsurface factors to determine the most suitable pre-drill hydrocarbon
45 column height distribution. This method contributes to reducing the largest source of
46 uncertainty, which in turn reduces the overall uncertainty associated with pre-drill
47 volume estimation. Such an approach will increase the accuracy of pre-drill volume
48 estimation, leading to more appropriate future development plans. We recommend

49 that the presented methods and lessons learnt are applied in basins settings
50 worldwide.

51 **1. Introduction**

52 Estimating pre-drill volumes is an essential part of the exploration process that
53 determines if a prospect contains a large enough volume of hydrocarbons to justify
54 drilling an exploration or appraisal well. Yet, despite its importance and an overall
55 improvement in available technology, the industry continues to be poor at estimating
56 pre-drill hydrocarbon volumes (Milkov, 2017). This is largely the result of uncertainty
57 associated with each of the ten main inputs required to calculate potential
58 hydrocarbon volumes (Table 1). Combining these inputs further compounds the level
59 of uncertainty resulting in errors, which can lead to surprises and often
60 disappointment once volumes are reassessed after drilling (Garb, 1988; Skaar et al.,
61 2000; Demirmen, 2007). Of all of the inputs, the hydrocarbon column height
62 uncertainty generally has the largest impact on the calculated pre-drill volume range
63 (Fig. 1). Despite this, efforts to constrain the column height are commonly bypassed
64 in favor of work that focuses on other inputs required to calculate pre-drill volumes
65 that carry far less uncertainty. Instead, we argue that constraining the hydrocarbon
66 column distribution should be prioritized for the benefit of reducing the overall
67 uncertainty of reserve estimation (Floris and Peersmann, 1998).

68 Hydrocarbon column heights have perhaps remained as one of the key uncertainties
69 in reserve calculations because of the difficulty in obtaining accurate empirical data.
70 Unlike some of the other input parameters such as porosity, the column height
71 cannot be calculated directly from well logs alone. Instead, three measurements are
72 required: the depth of the hydrocarbon-water contact (fluid contact), the structural

73 apex and the spill point (Fig. 2). The fluid contact can be estimated using well logs
74 and pressure data, however, calculation of the apex and spill point depths requires a
75 reliable top reservoir depth map, since the majority of exploration wells tend to be
76 drilled in down-flank positions. In turn, this requires access to 3D seismic data and a
77 velocity model for depth conversion. This data- and time-intensive approach may
78 explain why few studies of this kind have been carried out before.

79 A number of previous empirical reviews have measured hydrocarbon columns in
80 areas such as the Norwegian Continental Shelf (NCS), Malay Basin and Gulf of
81 Mexico, and all conclude that the observed column heights follow a lognormal
82 distribution (Fosvold et al., 2000; Niemann, 2000; Tanjung, 2014). This result is
83 largely representative of the type of distribution (Fig. 3A) that is widely used in oil and
84 gas exploration as a default for pre-drill volume estimation, regardless of the size of
85 the trap height or burial depth of the prospect. Two other types of commonly used
86 distributions are the normal distribution (Fig. 3B) and uniform distribution (Fig. 3C).
87 Deciding which distribution best describes the column height uncertainty has a
88 significant impact on the pre-drill volume range of a hydrocarbon prospect, and will
89 often determine whether an exploration well is drilled or not.

90 Using the geometry of a prospect to determine the pre-drill column height distribution
91 has only been incorporated into a handful of published studies. Graham et al. (2015)
92 concluded that integration of the trap height, genetic history and geological setting of
93 the prospect is likely to result in the most appropriate column height distribution.
94 Additional contributions by Schlömer and Krooss (1997) state the influence of area-
95 to-relief ratio on the potential discoverable hydrocarbon column. There is scope
96 therefore to introduce a new approach that directly links the pre-drill column height

97 distribution to the prospect's geometry, specifically the trap height and burial depth /
98 overburden thickness.

99 This piece of work is primarily concerned with presentation of the empirical data
100 collected across the NCS, as well as identifying trends and correlation between
101 subsets of the data. The 242 measured discoveries are located in a number of basins
102 spanning the Barents Sea, Norwegian Sea and Northern North Sea, and as such,
103 mix a range of different structural and stratigraphic settings. To explore the possible
104 underlying causes of the identified trends presented herein, the data would have to
105 be sub-divided allowing like-for-like basins to be compared. Subsequent technical
106 assessment of subsurface data covering each of the basins would require additional
107 time and methods, a process that demands its own study. It should also be noted
108 that the 242 data points analyzed for this study correspond to discovery cases only.
109 This study is primarily concerned with reducing the uncertainty in prediction of
110 hydrocarbon columns in success-case scenarios, therefore dry wells and causes of
111 failure fall outside the scope of work.

112 This study has three main aims. Firstly, to collect and present a large empirical
113 dataset of measured hydrocarbon column heights, associated trap heights, burial
114 depths, and trap-fill ratios for 242 discoveries across the NCS. Secondly, to identify
115 trends between the measured variables, and to analyze the role of trap-height and
116 burial depth on observed hydrocarbon column heights. Thirdly, to use the results of
117 such analysis to challenge common assumptions regarding column height probability
118 distributions.

119 **2. Study area and methodology**

120 The oil and gas discoveries used in this study are distributed across the NCS in three
121 different regions: the Barents Sea, the Norwegian Sea and the Northern North Sea
122 above 61°N (Fig. 4). Of the 242 discoveries, 123 are located in the Norwegian Sea,
123 81 in the Northern North Sea and 38 in the Barents Sea. The fields and associated
124 structural elements that have been measured as part of the study are summarized in
125 Table 2.

126 The NCS was selected for several reasons. Firstly, it is a good area to study the
127 relationship between trap geometry and hydrocarbon column heights because the
128 majority of the basins in the study areas have received plentiful hydrocarbon charge,
129 so charge limitation is not a significant issue (Doré and Jensen, 1996; Ostanin et al.,
130 2012; Hermanrud et al., 2014). For this reason, it is assumed that the observed
131 variations in column heights and trap-fill ratios are primarily a result of seal behaviour
132 and not because of a lack of charge (Hermanrud and Bols, 2002; Bolås and
133 Hermanrud, 2003; Halland et al., 2013). Secondly, the Norwegian Petroleum
134 Directorate (NPD) provides a large repository of well data, of which many details
135 become public two years after drilling and fully public after 20 years. Access to such
136 well-organized data is particularly helpful when ascertaining the fluid contact depth,
137 which can be directly taken from descriptions in the well reports or from pressure
138 data. Thirdly, the publically available seismic data covering the three regions has
139 been widely interpreted and a large number of good quality, top reservoir maps were
140 made available for this study. Maps were taken either from previous prospect
141 analyses or from regional maps, which were subsequently reinterpreted in more
142 detail where required.

143 Since the vast majority of the available seismic datasets are in the time domain, a
144 regional velocity cube was used to depth convert the top reservoir time (TWT) maps

145 into depth. Top reservoir depth maps were crosschecked against well tops to assess
146 if any depth shift was required. Access to such maps and well data ensures that the
147 relevant data required to calculate the column height, trap height and burial depth is
148 widely available across most of the NCS. However, the assimilation and quality
149 control of the data, which is necessary to measure the apex and spill point depths, is
150 more time consuming. Figure 5 shows an example of such data collection for
151 discovery wellbore 7121/7-1, which is part of the Snøhvit field in the southwestern
152 Barents Sea (Linjordet and Olsen, 1992). The top reservoir surface was mapped in
153 two-way-time, depth-converted and checked against the depth of the top reservoir in
154 the well. The fluid contact was taken from the publically available NPD fact pages
155 and crosschecked against observations and pressure measurements contained
156 within the final well report. The trap-fill ratio was then calculated based on what
157 proportion of the trap height was occupied by the hydrocarbon column (trap-fill ratio =
158 hydrocarbon column height / trap height).

159 As with all subsurface interpretation, and in particular depth conversion, we
160 acknowledge that there will be inaccuracies associated with the apex and spill point
161 depths for individual discoveries (Etris et al., 2001; Pon and Lines, 2005). However,
162 such inaccuracies are minimized in this study through local reinterpretation of
163 regional surfaces to increase topographic detail over the structures, as well as tying
164 the depth surfaces to the relevant well-tops after depth conversion. Consequently,
165 confidence in the collection methods and resulting dataset is good.

166 **3. Results**

167 The empirical data collected in this study is presented in a series of graphs that show
168 the range and distribution of measured variables, which includes the trap height,

169 burial depth, column height and trap-fill ratio for each discovery. Cross plots are
170 useful to identify potential correlations between particular variables and therefore
171 demonstrate possible controls on the observed hydrocarbon column heights. In
172 addition, trap-fill ratios calculated for each measured discovery are displayed as
173 proportionally sized data points on regional geological maps.

174 *3.1 Cross plots*

175 Figure 6A is a cross plot of hydrocarbon column height and trap height for all 242
176 data points with bordering histograms showing the distribution of data for each
177 variable. The density of data points decreases and becomes more sparsely
178 distributed as the trap height begins to exceed 400m and when column heights begin
179 to exceed 300m, which is shown by a broadening of the 95% confidence interval of
180 the regression line, indicated by the shading. The R-value (the correlation coefficient
181 between the two-plotted variables) of 0.86 indicates that there is a strong positive
182 correlation between trap height and hydrocarbon column height. The linear dashed
183 line on Figure 6A represents the one-to-one relationship between trap height and
184 column height. All points that fall on this line have a trap-fill of 100%, and the
185 structures are considered to be “filled-to-spill”. Figure 6B is a cross plot of the
186 hydrocarbon column height and burial depth / overburden thickness. Burial depth
187 values are distributed centrally with the density of data points decreasing towards
188 very low and very high values. The number of hydrocarbon columns recorded in
189 structures with burial depths exceeding 4000m is limited, which is shown by the
190 broadening of the 95% confidence interval either side of the regression line. The R-
191 value of 0.31 shows there is a moderate positive correlation between burial depth
192 and hydrocarbon column height.

193 Figure 7 displays three trap height versus hydrocarbon column height cross plots
194 (Figs. 7A-C) and three burial depth versus hydrocarbon column height cross plots
195 (Figs. 7D-F) for each of the three regions covered by this study. All three regions
196 show a strong positive correlation between hydrocarbon column height and trap
197 height with the corresponding R-values varying between 0.76 (Barents Sea) and 0.88
198 (Norwegian Sea). Note the difference in measured trap heights across the three
199 regions. In the Northern North Sea and Norwegian Sea they reach up to 700m,
200 whereas the maximum trap height observed in the Barents Sea is just over 400m.
201 Figures 7D-F show a weak to moderate positive correlation between burial depth and
202 column height. The Northern North Sea has the lowest R-value of 0.16 and the
203 Barents Sea has the highest at 0.47. Again, note the difference in the range of burial
204 depths across the three regions. Hydrocarbon columns measured in the Northern
205 North Sea and Norwegian Sea are buried between 1000 and 5000m. However, in the
206 Barents Sea the discoveries are buried at shallower depths, between 200 and
207 3000m. The maximum hydrocarbon column observed in the Northern North Sea is
208 452m (well 34/8-7), 680m in the Norwegian Sea (Åsgard discovery) and 296m in the
209 Barents Sea (Iskrystall discovery).

210 *3.2 Spatial distribution of trap-fill*

211 Trap-fill ratio, a measure of how much of the trap height is occupied by the
212 hydrocarbon column, is represented in three maps in Figure 8. Each colored,
213 proportionally sized circle represents the trap-fill ratio for each discovery. The
214 Barents Sea (Fig. 8A) contains a broad range of trap-fill ranges, particularly in the
215 Hammerfest Basin, which contains discoveries with all ranges of trap-fill. 100% trap-
216 fill is most prevalent at the basin margins. The other major cluster of discoveries is
217 located on the Polhem Sub-platform, where the measured structures range from 50

218 to 100% filled. Figure 8B shows the distribution of observed trap-fill ratios in the
219 Norwegian Sea. There is a dense clustering of data points along the axis of the
220 Revfallet Fault Complex, which borders the Halten and Donna Terrace. The majority
221 of the discoveries have a trap-fill ratio of 75% or more, with a few interspersed
222 discoveries with lower levels of trap-fill. The cluster of points on the Nyk High, close
223 to the Aasta Hansteen field, shows that most discoveries in this area tend to be
224 100% filled. Figure 8C shows the trap-fill distribution across the Northern North Sea.
225 Similar to the Norwegian Sea, the majority of discoveries are filled-to-spill, however,
226 they are more widely distributed and tend to be located more closely to discoveries
227 with lower trap-fill ratios of between 50 and 75%, for example on the Lomre Terrace
228 and Tampen Spur.

229 **4. Data analysis**

230 The empirical dataset was evaluated using a forward probability model, otherwise
231 known as a forward probability-tree, which required each input variable (trap height
232 and burial depth) and output variable (trap-fill ratio) to be categorized into a series of
233 discrete bins. A 3x3 probability distribution matrix is then populated by the forward
234 probabilities calculated in the probability tree to assess how the trap fill ratio varies
235 with trap height and burial depth. A more detailed explanation of this workflow is
236 described below.

237 *4.1 Forward probability model*

238 A forward probability or 'decision tree' approach is a useful tool to assess what
239 influence (if any) the trap height and burial depth have on the trap-fill ratio, and to see
240 if the relationship between them can be used in a predictive manner. The method
241 was chosen to display the distribution of trap-fill ratios for different ranges of trap

242 height and burial depth. The number of bins that define the output variable, in this
243 case, the trap-fill ratio, defines the first set of branches in the forward probability tree
244 (Fig. 9). The number of bins associated with each input variable, i.e. the trap height
245 and burial depth, determine the number of branches that define the second and third
246 decision levels. The total number of branches is equal to the product of the number
247 of bins for each input and output variable, multiplied together. Once the tree has
248 been populated, the probability for each calculated outcome is normalized against
249 other outcomes that share similar trap height and burial depth values. This
250 normalization step is necessary to calculate the probability of finding a given trap-fill
251 ratio for each combination of trap height and burial depth values.

252 *4.2 Binning the data*

253 A number of methods can be used to calculate a suitable number of bins for a given
254 dataset (Miller, 1989; Wand, 1997). One of the simplest approaches is to set the
255 number of bins equal to the square root of the total number of values in the dataset,
256 otherwise known as the square-root choice method. This gives approximately 15 bins
257 of equal width for each variable, as illustrated in Figures 10A-C. However, using 15
258 bins for each of the three variables in a probability tree would result in 3375
259 probabilities ($15 \times 15 \times 15$), which far exceeds the actual size of the dataset (242). For
260 the purpose of this study, it is necessary to cap the number of bins to avoid such a
261 large number of probabilities. Each variable is therefore divided into just five bins of
262 equal width as shown in Figures 10D-F. This has the desired result of reducing the
263 number of possible outcomes to 125 ($5 \times 5 \times 5$). However, because of the irregular
264 distribution of values across each variable, some bins contain very few or no values
265 at all. This becomes problematic when calculating probabilities for certain
266 combinations of trap-fill, burial depth and trap height, with too many zero probabilities

267 being returned. To avoid this issue, bins of variable width must be used in order to
268 allow the number of values to be more evenly redistributed across each bin (Figs
269 10G-I) (Miller, 1989).

270 Burial depth was divided into three bins: 0-1500m, 1501-3000m and >3000m (Fig
271 10G), and the trap height was also divided into three bins: 0-150m, 151-300m and
272 >300m (Fig. 10H). The trap-fill ratio was divided into four bins corresponding to 0-
273 50%, 51-75%, 75-99% and 100% trap-fill (Fig. 10I). 100% trap fill is assigned its own
274 bin since nearly half of the measured discoveries (111/242) recorded this level of
275 trap-fill (Fig. 9). Relatively few discoveries had trap-fill values of 50% or lower
276 (31/242), so this category was not further subdivided. The total number of bins gives
277 a workable number of 36 possible outcomes (4x3x3), with only two out of the 36
278 outcomes having a zero probability. These two zero probability outcomes are both
279 caused by a lack of discoveries where the trap-fill exceeds 75% in structures with
280 trap heights above 300m and burial depths of less than 1500m (Fig. 9).

281 *4.3 Probability distribution matrix*

282 The 3x3-output matrix (Fig. 11) shows how the normalized trap-fill probabilities,
283 calculated in the forward-probability tree, vary across different trap height and burial
284 depth ranges. The observed distribution of trap-fill probabilities does not follow the
285 same pattern for each burial depth and trap height combination and as such, there is
286 not one type of distribution that describes all nine input scenarios. The bullet points
287 below describe the other key observations:

- 288 • When the trap height is 150m or less (at all burial depths), the probability of 0-99%
289 trap-fill is consistently low, whereas the probability of 100% trap-fill is very high.

290 Furthermore, the probability of recording 100% trap-fill is approximately twice as
291 likely as recording a trap-fill ratio between 0 and 99%.

292 • For trap heights between 151 and 300m, the distribution of trap-fill ratio is less
293 consistent at different burial depths. When the burial depth is 1500m or less, the
294 most likely trap-fill range is between 51 and 75% and the least likely trap-fill is
295 100%. However, when the burial depth exceeds 1500m, this pattern is reversed
296 and 100% trap-fill becomes the most likely outcome, whilst 0-50% trap-fill
297 becomes the least likely.

298 • For trap heights exceeding 300m with a burial depth of less than 1500m, 0-50%
299 trap-fill is most likely and there are no discoveries with a trap-fill ratio above 75%.
300 Discoveries with trap heights exceeding 300m at depths of 1501-3000m are most
301 likely to have a trap-fill ratio of 51-75% and least likely to have 100% trap-fill.
302 However, when the burial depth exceeds 3000m, 100% becomes the most likely
303 trap-fill ratio and 0-50% the least likely.

304 To summarize, two main trends are observed. Firstly, as the trap height increases for
305 a given burial depth, the probability of 100% trap-fill progressively decreases and the
306 probability of 0-50% trap-fill progressively increases. Secondly, as the burial depth
307 increases for a given trap height, the probability of 100% trap-fill increases, whilst the
308 probability of 0-50% trap-fill decreases. These reversals in trap-fill ratio distributions
309 are evident across all trap height categories for a given burial depth and for all burial
310 depths for a given trap height.

311 **5. Discussion**

312 *5.1 Determining pre-drill hydrocarbon column height distributions*

313 Across all three regions of the NCS, there is a strong positive correlation between the
314 hydrocarbon column height and trap height. Although it may seem obvious, it is
315 important to recognize that trap height exerts a significant control on the hydrocarbon
316 column when estimating pre-drill column heights. Geometrically, a high-relief
317 structure is more likely to be able to hold a taller hydrocarbon column than a low-
318 relief structure. However, a high-relief structure at shallow depths is significantly less
319 likely to be filled-to-spill than those at greater depths (Fig. 11). A weaker positive
320 correlation exists between the column height and burial depth suggesting that the
321 burial depth exerts some control on column heights, but that the relationship between
322 these variables is more complicated. The correlation between column height and
323 burial depth appears to be strongest in shallower discoveries, as shown by the
324 relatively high correlation coefficient for the Barents Sea (Fig. 7).

325 The 3x3 matrix (Fig. 11) clearly shows that the observed distribution of trap-fill ratios
326 does not stay constant for all combinations of trap height and burial depth. In order to
327 reflect this in the pre-drill volume estimation, the burial depth and height of a prospect
328 should be taken into consideration when selecting the type of probability distribution
329 to use for the hydrocarbon column height. The observed trap-fill ratios for discoveries
330 in trap heights of 150m or less at all burial depths suggest that a strongly negatively
331 skewed distribution is most appropriate for prospects in low-relief structures. A
332 negatively skewed distribution remains applicable when the trap height increases to
333 between 151 and 300m at burial depths of 1500m or more. However, for intermediate
334 trap heights at depths of less than 1500m and for trap heights exceeding 300m with
335 less than 3000m of burial depth, the probability distribution curve should be positively
336 skewed in order to reflect the higher probability of a lower trap-fill ratio.

337 These observations challenge the widely accepted view that the hydrocarbon column
338 should always follow a log normal distribution (Fosvold et al., 2000; Niemann, 2000;
339 Demirmen, 2007). Integration of this approach with other existing methods for column
340 height prediction (e.g. fault seal analysis and buoyancy pressure calculations) should
341 lead to improved estimation of pre-drill hydrocarbon volumes by reducing the
342 prevalence of under- and over-estimation of the hydrocarbon column height in
343 prospect analysis.

344 *5.2 The benefits of using integrative methods*

345 It has been acknowledged that when exploration and production companies integrate
346 a variety of probabilistic methods into their workflows and include base-rate figures,
347 their competitive position tends to improve (Jonkman et al., 2000; Skarr et al., 2002;
348 Milkov, 2017). Adopting this approach when determining appropriate hydrocarbon
349 column distributions is particularly important since it has been widely acknowledged
350 as being the most significant contributor to uncertainty in pre-drill volume prediction.
351 For this reason, acquisition and assessment of hydrocarbon column data will have
352 the largest impact on reducing the overall uncertainty (Floris and Peersmann, 1998;
353 Demirmen, 2007). However, this approach should not replace the need for detailed
354 prospect and trap specific analysis (Graham et al., 2015). Thorough analysis of the
355 structural and stratigraphic components of a prospect is always recommended for
356 meaningful risking and decisions that are taken during drill or drop, or appraisal
357 assessments. Best practice lies in integrating the probability- and geological-based
358 approaches to create a multi-disciplinary workflow for improved assessment of
359 hydrocarbon column uncertainty, and thus improved pre-drill volume prediction.

360 *5.3 Universal implications*

361 The data used in this study is collected from a range of basins located on the NCS.
362 Nevertheless, we recommend that the trends and lessons learnt in this study be
363 applied to basins and prospects that lie outside the NCS. The hydrocarbon column
364 height distribution will always remain an uncertainty when calculating pre-drill
365 volumes, regardless of where the prospect is located. This approach also has the
366 wider benefit of improving the efficiency of the exploration and production of
367 hydrocarbons, which will ultimately help to drive down costs. Improved placement of
368 wildcat, appraisal and development wells will lead to a reduction in the number of
369 redundant wells, helping to reduce emissions that are emitted during the drilling
370 process. This in turn will reduce the negative impact of drilling on the environment,
371 which is timely given the oil and gas industry is increasingly seeking ways to improve
372 its environmental image.

373 *5.4 Future work*

374 This study strongly suggests that burial depth and trap height is used to guide trap-fill
375 and hydrocarbon column height prediction. However, the observed patterns could be
376 strengthened or challenged when more values are added to the dataset. A lack of
377 values, for example in discoveries with trap heights above 300m in burial depths of
378 less than 1500m, may weaken the strength of the observed pattern, but may also be
379 indicative of the type of trap geometries that are encountered at different depths in
380 the subsurface. The same approach should be extended further south on the NCS
381 and into the UK Continental Shelf (UKCS). Where possible, it is recommended that
382 additional data are collected further afield, for example from the Gulf Coast, to
383 investigate if different basins settings influence trap fill distributions across variable
384 trap heights and burial depths. Addition of more data points to the dataset will

385 increase the statistical significance of the results and further improve its power as a
386 tool for guiding pre-drill column height predictions.

387 **6. Summary and conclusions**

388 This study presents an empirical dataset across the NCS that includes
389 measurements of the trap height, burial depth, hydrocarbon column and trap-fill ratio
390 of 242 fields and discoveries. To the best of the authors' knowledge, this is the first
391 study of its kind. The key findings from this work are summarized below:

- 392 • Simple statistical analysis of the dataset reveals a strong correlation between
393 trap height and hydrocarbon column height, and a weaker correlation between
394 burial depth and hydrocarbon column height.
- 395 • A forward probability approach was used to calculate the probability of a given
396 trap-fill ratio for different combinations of trap height and burial depth ranges. The
397 results are visualized in a 3x3 matrix, which can be used to demonstrate the
398 distribution of trap-fill ratios in discoveries with similar trap heights and burial
399 depths.
- 400 • The distribution of trap-fill ratios does not stay constant across all trap height and
401 burial depth ranges. When the trap height starts to increase, for a given burial
402 depth, the probability of 100% trap-fill diminishes and the probability 0-50% trap-
403 fill increases. Similarly, as the burial depth increases for any given trap height,
404 the probability of 100% trap-fill increases whilst the probability of 0-50% trap-fill
405 decreases.
- 406 • Pre-drill column height prediction should be adjusted according to the geometry
407 and burial depth of the prospect, rather than applying a fixed statistical
408 distribution to all prospects. Integration of this empirical approach with

409 consideration of trap-specific details can make a significant contribution to
410 improving the predictability of hydrocarbon column heights in undrilled prospects.
411 This, in turn, will help to reduce the overall uncertainty associated with pre-drill
412 volume estimation in exploration.

- 413 • This method of data collection and analysis should be repeated for more
414 discoveries across the NCS and the neighboring UKCS. Inclusion of data from
415 different hydrocarbon provinces, such as the Gulf Coast would also help to
416 increase the size and geographical spread of the dataset. This leads to more
417 meaningful statistical outcomes and enhances the predictive power of the
418 dataset.
- 419 • Estimation of the hydrocarbon column remains a constant uncertainty when
420 assessing pre-drill volumes for all prospects, regardless of location. It is therefore
421 recommended that data collections methods and lessons learnt from this study
422 are applied universally, and integrated into current methods that are used to
423 estimate pre-drill hydrocarbon column heights for prospects worldwide.

424

425 **References**

426 Bolås, H.M.N. and Hermanrud, C., 2003, Hydrocarbon leakage processes and trap
427 retention capacities offshore Norway: *Petroleum Geoscience*, v. 9, no. 4, p. 321-332,
428 doi:10.1144/1354-079302-549.

429 Demirmen, F., 2007, Reserves estimation: the challenge for the industry: *Journal of*
430 *Petroleum Technology*, v. 59, no. 5, p. 80-89, doi:10.2118/103434-JPT.

431 Doré, A.G. and Jensen, L.N., 1996, The impact of late Cenozoic uplift and erosion on
432 hydrocarbon exploration: offshore Norway and some other uplifted basins: *Global*
433 *and Planetary Change*, v. 12, no. 1-4, p. 415-436, doi:10.1016/0921-8181(95)00031-
434 3.

435 Etris, E.L., Crabtree, N.J., Dewar, J. and Pickford, S., 2001, True depth conversion:
436 more than a pretty picture: *CSEG recorder*, v. 26, no. 9, p. 11-22.

437 Floris, F.J. and Peersmann, M.R., 1998, Uncertainty estimation in volumetrics for
438 supporting hydrocarbon exploration and production decision-making: *Petroleum*
439 *Geoscience*, v. 4, no. 1, p. 33-40, doi:10.1144/petgeo.4.1.33.

440 Fosvold, L., Thomsen, M., Brown, M., Kullerud, L., Ofstad, K. and Heggland, K.,
441 2000, Volumes before and after exploration drilling: results from the project:
442 *Evaluation of Norwegian Wildcat Wells (Article 2): Norwegian Petroleum Society*
443 *Special Publications*, v. 9, p. 33-46, doi:10.1016/S0928-8937(00)80007-7.

444 Garb, F.A., 1988, Assessing Risk in Estimating Hydrocarbon Reserves and in
445 Evaluating Hydrocarbon-Producing Properties: *Journal of Petroleum Technology*, v.
446 40, no. 6, p. 765-778, doi:10.2118/15921-PA.

447 Graham, C.B., Savrda, A.M., Davis, S., Walker, P.E., Sykes, M.A. and Corona, F.V.,
448 2015, Improving Hydrocarbon Column Height Estimates: Results From a Global
449 Synthesis (abs): AAPG Search and Discovery article 90216, accessed August 20th,
450 2019,
451 <http://www.searchanddiscovery.com/abstracts/html/2015/90216ace/abstracts/208845>
452 0.html

453 Halland, E.K., Mujezinović, J., Riis, F., 2013, CO2 Storage Atlas, Barents Sea,
454 accessed September 2nd, 2019, <https://www.npd.no/en/facts/publications/>.

455 Hermanrud, C. and Bols, H.M.N., 2002, Leakage from overpressured hydrocarbon
456 reservoirs at Haltenbanken and in the northern North Sea: Norwegian Petroleum
457 Society Special Publications, v. 11, p. 221-23, doi:10.1016/S0928-8937(02)80017-0.

458 Hermanrud, C., Halkjelsvik, M.E., Kristiansen, K., Bernal, A. and Strömbäck, A.C.,
459 2014, Petroleum column-height controls in the western Hammerfest Basin, Barents
460 Sea: Petroleum Geoscience, v. 20, p. 227-240, doi:10.1144/petgeo2013-041.

461 Jonkman, R. M., Bos, C. F. M., Breunese, J. N., Morgan, D. T. K., Spencer, J. A., and
462 Søndena, E. 2000, Best Practices and Methods in Hydrocarbon Resource
463 Estimation, Production and Emissions Forecasting, Uncertainty Evaluation and
464 Decision Making; Society of Petroleum Engineers, doi:10.2118/65144-MS

465 Linjordet, A. and Olsen, R.G., 1992, The Jurassic Snøhvit Gas Field, Hammerfest
466 Basin, Offshore Northern Norway: AAPG Special Volume, M54: Giant Oil and Gas
467 Fields of the Decade 1978-1988, Chapter 22, p. 349-370.

468 Milkov, A.V., 2017, Integrate instead of ignoring: Base rate neglect as a common
469 fallacy of petroleum explorers: AAPG Bulletin, v. 101, p. 1905-1916, doi:
470 10.1306/0327171622817003.

471 Miller, J.C., 1989, Statistics for advanced level: Cambridge University Press., 442 p.

472 Niemann, J.C., 2000, Statistical Distributions of Hydrocarbon Column Heights for
473 Gulf of Mexico Trap Types and Seals (abs): AAPG Discovery series No. 1, last
474 accessed 18th September 2019,
475 <http://archives.datapages.com/data/specpubs/discovery1/D0127/D0127001.HTM>.

476 Norwegian Petroleum Directorate, 2019, Factpages and Factmaps, accessed 30th
477 August 2019, https://factmaps.npd.no/arcgis/rest/services/FactMaps/3_0/MapServer.

478 Ostanin, I., Anka, Z., di Primio, R. and Bernal, A., 2012, Identification of a large
479 Upper Cretaceous polygonal fault network in the Hammerfest basin: Implications on
480 the reactivation of regional faulting and gas leakage dynamics, SW Barents
481 Sea: Marine Geology, v. 332, p. 109-125, doi:10.1016/j.margeo.2012.03.005.

482 Pon, S. and R. Lines, L., 2005, Sensitivity analysis of seismic depth migrations:
483 Geophysics, v. 70, p. S39-S42, doi:10.1190/1.1897036.

484 Schlömer, S. and Krooss, B.M., 1997, Experimental characterisation of the
485 hydrocarbon sealing efficiency of cap rocks: Marine and Petroleum Geology, v. 14, p.
486 565-580, doi:10.1016/S0264-8172(97)00022-6.

487 Skaar, K.J., Spencer, A.M., Alexander-Marrack, P. and Støle, G., 2000, Suggestions
488 for an improved exploration process - lessons from the project: Evaluation of
489 Norwegian Wildcat Wells (Article 4): NPF Special Publication no. 9, p. 57-63.

490 Tanjung, B.A., 2014, Statistical Distributions of Hydrocarbon Column Heights for
491 Determining Acreage of Prospect to Estimate Hydrocarbon Resources in Kakap
492 Block (abs), last accessed August 12th 2019,
493 http://archives.datapages.com/data/ipa_pdf/2014/IPA14-G-173.htm

494 Wand, M.P., 1997, Data-Based Choice of Histogram Bin Width: The American
495 Statistician, v. 51, p. 59-64, doi:10.1080/00031305.1997.10473591.

496

497 **Table. 1** A list of defined inputs that are required to calculated hydrocarbon volumes

498

Input	Definition
Hydrocarbon column height	The height of a continuous hydrocarbon column measured from the apex of the structure down to the hydrocarbon-water contact
Recovery factor	The percentage of hydrocarbons that can be produced from the volume of hydrocarbons initially in place
Net/gross ratio	The reservoir rock thickness that has sufficient porosity/permeability from which hydrocarbons can be produced divided by the total reservoir thickness (see below for definition)
Gas fraction of column height	Proportion of the hydrocarbon column height occupied by gas
Porosity (effective)	Interconnected space within the rock that can be occupied by moveable fluids. Excludes isolated pore spaces.
Reservoir thickness	Thickness of the stratigraphic unit that contains the reservoir beds
Oil saturation	Fraction of the pore space occupied by oil
Area	Areal extent of the reservoir contained within the closure at the depth of the fluid contact
Formation volume factor (oil)	The oil volume at reservoir conditions divided by the oil volume at standard conditions (surface conditions)
Depth-dependent area	Function that describes the relationship between depth and the areal extent of the reservoir contained within the closure

499 **Table 2.** A list of structural elements, and fields and discoveries that have been
 500 measured in this study

Region	Structural elements	Fields and Discoveries
Barents Sea	Hammerfest Basin, Loppa High, Måsøy Fault Complex, Nysleppen Fault Complex, Polhem Sub-Platform, Troms-Finmark Fault Complex	Alke, Bamse, Goliat, Iskrystall, Johan Castberg, Nucula, Norvarg, Snøhvit, Wisting
Norwegian Sea	Dønna Terrace, Halten Terrace, Nyk High, Rås Basin, Vøring Basin,	Aasta Hansteen, Åsgard, Alve, Bauge, Draugen, Dvalin, Fenja, Heidrun, Hyme, Kristin, Linnorm, Maria, Marulk, Mikkel, Morvin, Njord, Norne, Ormen Lange, Skarv, Skuld, Trestakk, Tyrihans, Urd, Ærfugl
Northern North Sea	Gullfaks Block Zone, Lomre Terrace, Marflo Spur, Måloy Slope, Tampen Spur, Tjalve Terrace, Uer Terrace	Byrding, Fram, Gjøa East, Gjøa, Gullfaks, Gullfaks Sør, Knarr, Kvitebørn, Snorre, Stafjord, Stafjord Nord, Stafjord Øst, Sygna, Tordis, Tordis Borg, Tordis Øst, Vega, Vega South, Valemon, Vigdis, Vigdis Sørøst, Vigdis West, Visund

501

502 **Figure captions**

503 **Fig.1.** A typical tornado plot generated during pre-drill volume estimation (oil case). It
504 shows the sensitivity of the calculated hydrocarbon reserves to changes in the input
505 variables. Changes in the hydrocarbon column height has the largest effect of all the
506 inputs for the majority of exploration prospects. P10 (possible) means that there is at
507 least a 10% probability that the actual volume of hydrocarbons recovered equals or
508 exceeds the P10 estimate (high estimate). P90 (proved) means that there is at least
509 a 90% probability that the actual volume of hydrocarbons recovered equals or
510 exceeds the P90 estimate (low estimate). Input data are sourced from the NCS.

511 **Fig. 2.** A schematic diagram of a fault-bounded hydrocarbon trap. The depth of the
512 structural apex, fluid contact and spill point must be measured in order to calculate
513 the following dimensions: burial depth (a), hydrocarbon column height (b) and trap
514 height (c).

515 **Fig. 3.** Three different types of probability distributions. (A) shows a lognormal
516 distribution, which is recognized by a skewed profile that is characterized by an initial
517 steeply dipping limb leading to a peak followed by a longer more gradual dipping
518 limb. (B) shows a normal distribution, which is typically symmetrical about x when x is
519 equal to the mean and (C) shows a uniform distribution, in which all values are
520 equally probable.

521 **Fig. 4.** A map of the Norwegian Continental Shelf showing the locations of discovery
522 boreholes used in this study. The distribution of boreholes is separated into three
523 regions: the Barents Sea, the Norwegian Sea and the Northern North Sea (above
524 61°N). The geological structural base map is from the Norwegian Petroleum
525 Directorate (NPD FactMaps, 2019).

526 **Fig. 5.** An example of measurements taken from a structure targeted by exploratory
527 well 7121/7-1, in the Snøhvit field in the southwest Barents Sea. (A) is the map of the
528 top reservoir (Stø Fm.) and indicates the location of cross section A-A' in white, the
529 gas-water contact contour (red) and the spill-point contour (black). (B) shows cross
530 section A-A' with seismic and (C) shows cross section A-A' without seismic. The spill
531 point, gas-water contact and apex depths, which are required to calculate the
532 hydrocarbon column height, trap height, trap-fill ratio and burial depth of the
533 discovery are marked on (B)-(C).

534 **Fig. 6.** Cross plots of the empirical data. (A) is a cross plot of the trap height and
535 hydrocarbon column height for all measured discoveries. The linear dashed line
536 represents discoveries that record 100% trap-fill and are referred to as 'filled-to-spill'.
537 All points below this line indicate the structure is underfilled. (B) is a cross plot of the
538 burial depth and hydrocarbon column height. Bordering histograms on the x- and y-
539 axes show the distribution of each variable. Both graphs display a blue regression
540 line bordered by a shaded area. The strength of each correlation coefficient is
541 indicated by the rvalue and the shading indicates the 95% confidence interval of the
542 regression line's location.

543 **Fig. 7.** Six cross plots for each of the three regions across the Norwegian Continental
544 Shelf. The hydrocarbon column height is plotted against trap height for the Northern
545 North Sea (A), Norwegian Sea (B) and Barents Sea (C). The hydrocarbon column
546 height is plotted against the burial depth for the Northern North Sea (D), Norwegian
547 Sea (E) and Barents Sea (F). Regression lines plotted on each graph indicate the
548 line of best fit and the accompanying rvalue indicates the strength of the correlation

549 coefficient between the two variables. Shading either side of the regression line
550 represents the 95% confidence interval of the regression line's location.

551 **Fig. 8.** Spatial distribution of trap-fill ratios for each measured discovery across the
552 Barents Sea (A), Norwegian Sea (B) and Northern North Sea (C). The larger and
553 darker colored the circle, the higher the trap fill ratio, as shown by the largest dark
554 red circle, which represents 100% trap fill. The base map is a structural map outlining
555 the main geological elements (NPD FactMaps, 2019).

556 **Fig. 9.** A decision tree, which is used to estimate the probability of encountering a
557 particular trap-fill ratio, given the trap height and burial depth of the structure is
558 known. The trap-fill ratio is the outcome variable and defines the first decision level. It
559 is divided into four branches and the values associated with each branch is defined
560 by the bin widths in Fig. 10I. The subsequent second and third decision levels are
561 defined by the two input variables: the trap height and burial depth. The trap height
562 defines the second decision level, which is divided into three branches. The values
563 associated with each branch are shown by the bins widths in Fig. 10H. The burial
564 depth defines the third decision level and is divided into three branches. The values
565 for each branch are defined by the bins widths in Fig. 10G. The decision tree
566 contains 36 different probable outcomes. Each outcome carries an absolute
567 probability and a normalized probability. The absolute probability is the product of
568 three probabilities, each one associated with one branch at decision level one, two
569 and three. The normalized probability is the absolute probability normalized against
570 other absolute probabilities that share the same trap height and burial depth ranges.
571 There are nine different trap height/burial depth combinations in total.

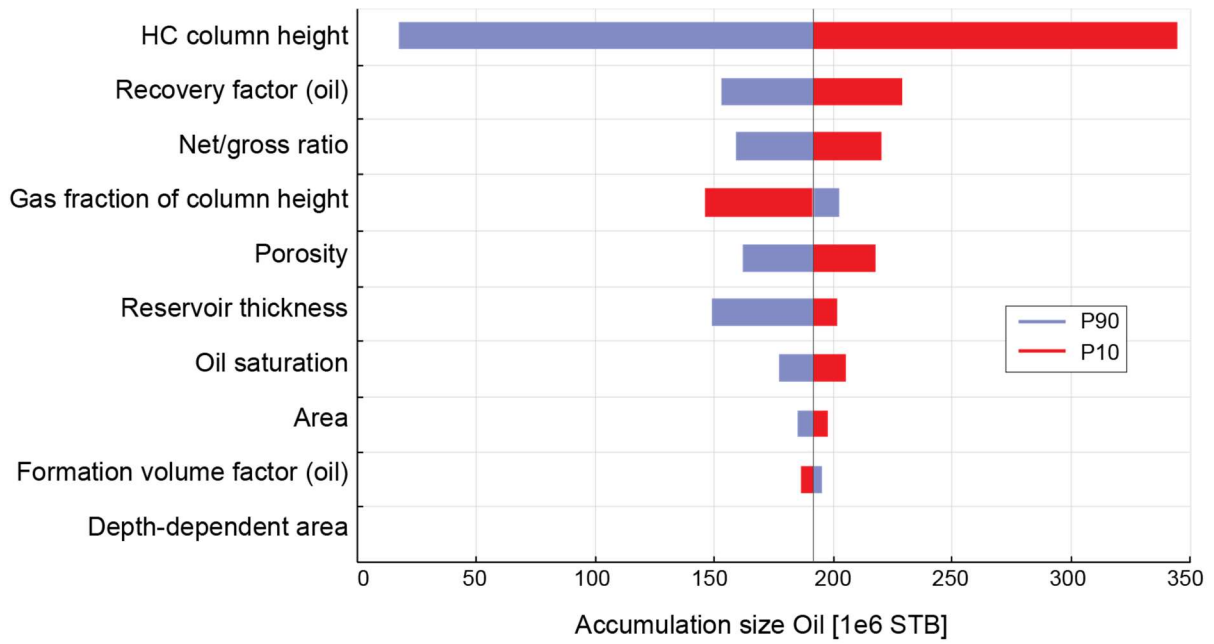
572 **Fig. 10.** A series of bar charts showing the distribution of the burial depths (dark
573 blue), trap heights (medium blue) and trap-fill ratios (light blue) for all measured
574 discoveries across the NCS. (A), (B) and (C) splits each dataset into 15 equally
575 spaced bins. (D) (E) and (F) divides each dataset in into five equally spaced bins. (G)
576 divides the burial depth dataset into three bins of unequal width. (H) divides the trap
577 height dataset into three bins of unequal width and (I) divides the trap fill ratio dataset
578 into four bins of unequal width. The bins widths chosen in (G), (H) and (I) determine
579 the number of branches in the decision tree shown in Fig. 9.

580 **Fig. 11.** A three by three probability distribution matrix showing how the probability of
581 different trap fill ratios changes when the trap height and burial depth dimensions
582 vary. Each sub-chart represents the distribution of trap-fill ratio probabilities for each
583 of the nine burial depth (y-axis) and trap height (x-axis) combinations. The nine sub-
584 charts are populated using the normalized probabilities calculated in Fig. 9. The
585 number of measured discoveries in the dataset that corresponds to one of the nine
586 trap height/burial depth combinations is indicated by n.

587

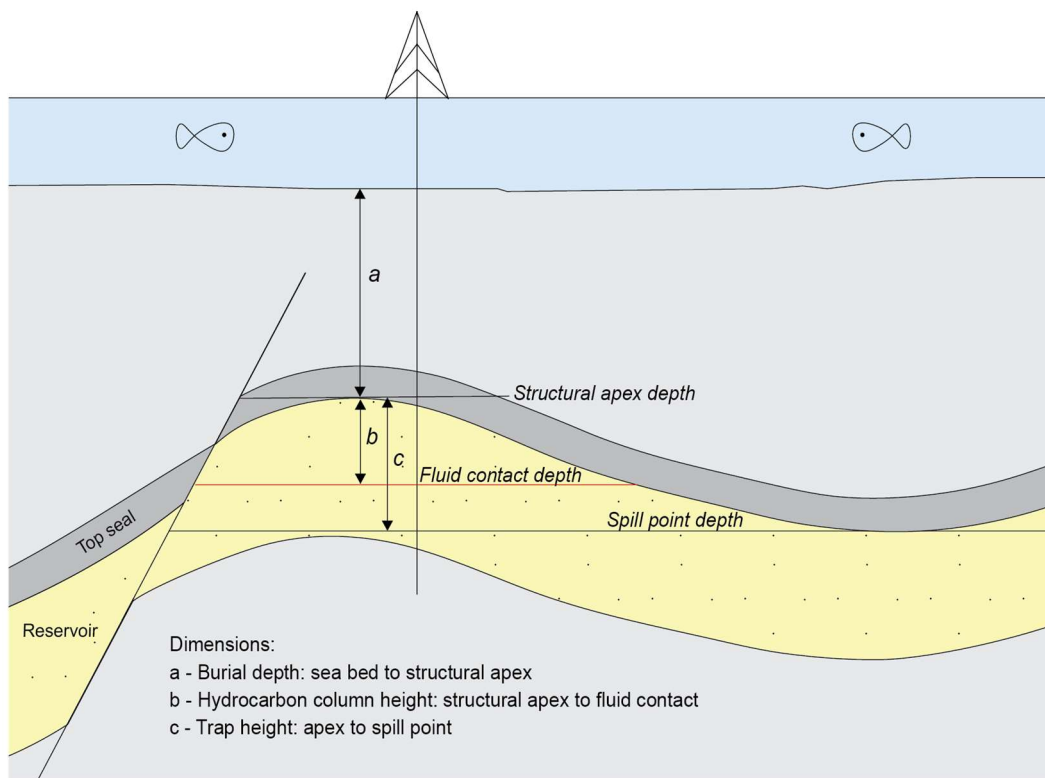
588 **Figures**

589 Figure 1



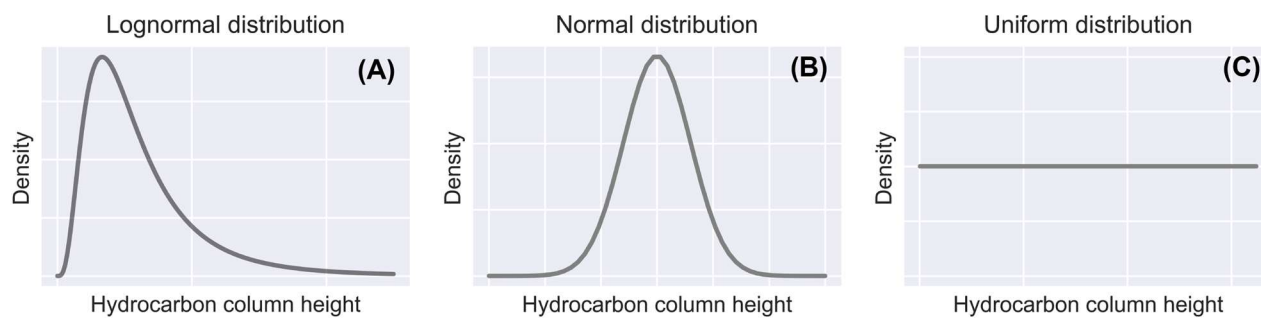
590

591 Figure 2



592

593 Figure 3



594

595

596

597

598

599

600

601

602

603

604

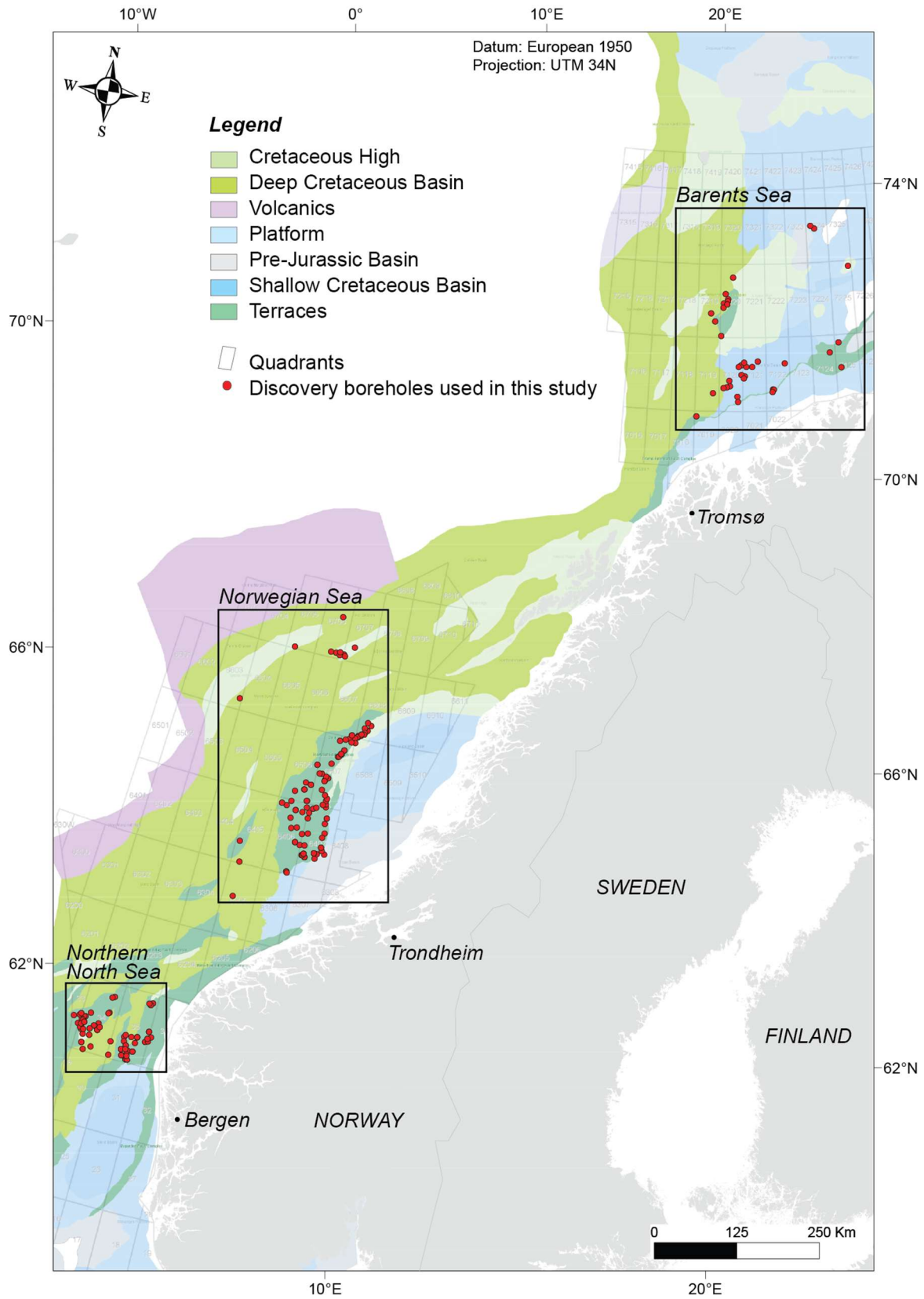
605

606

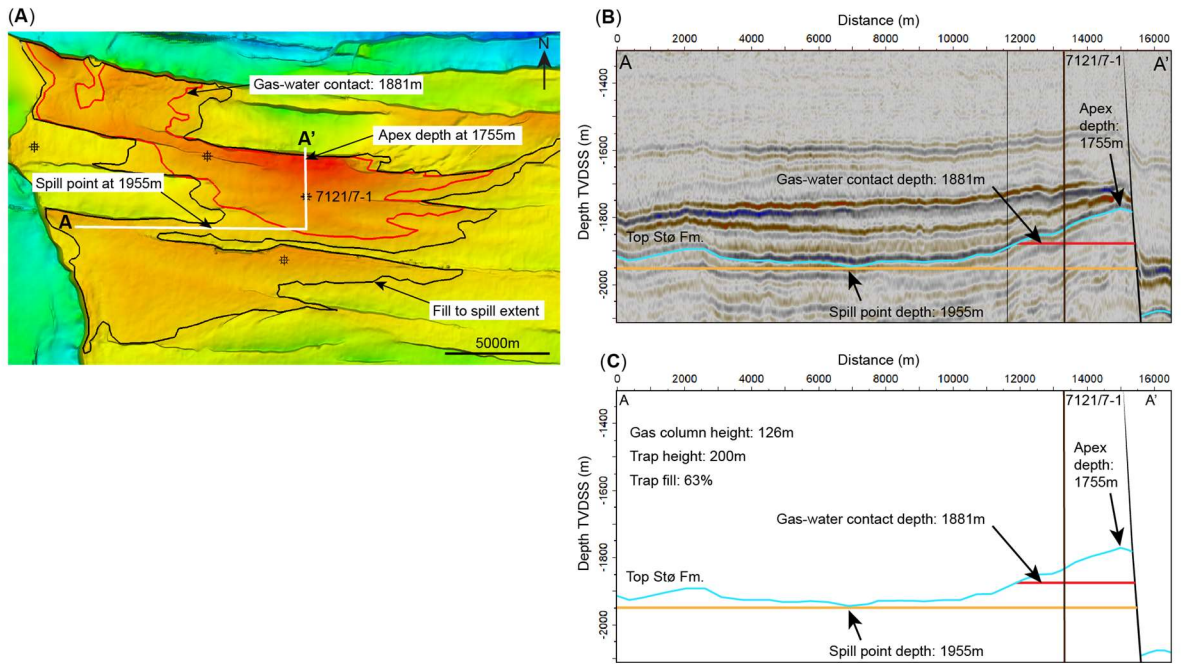
607

608

609 Figure 4



611 Figure 5



612

613

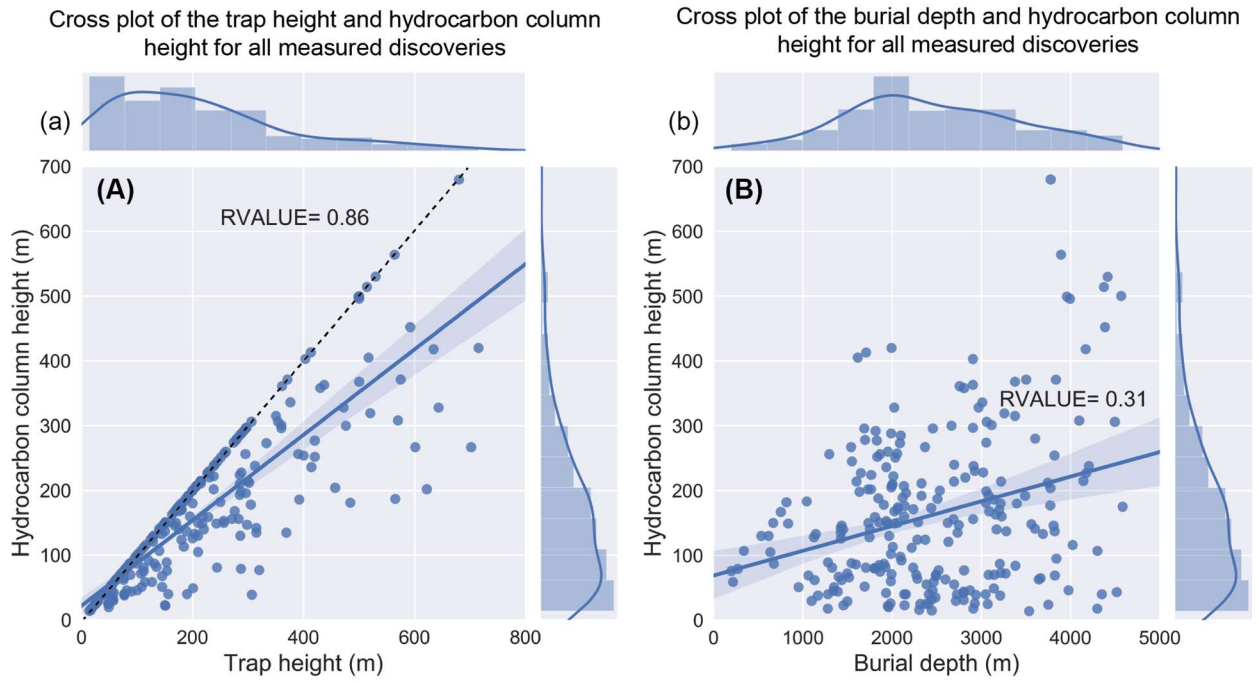
614

615

616

617

618 Figure 6



619

620

621

622

623

624

625

626

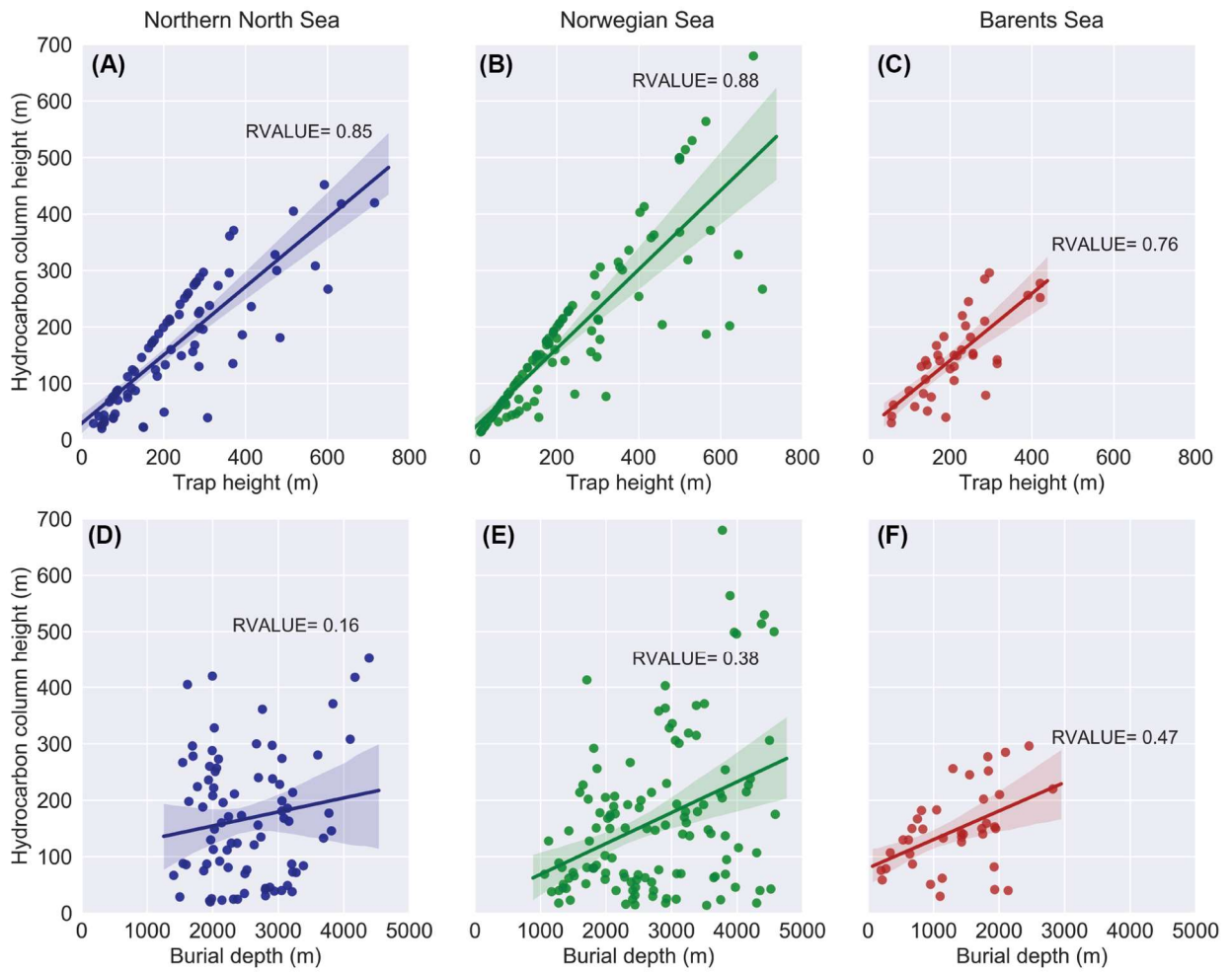
627

628

629

630

631 Figure 7



632

633

634

635

636

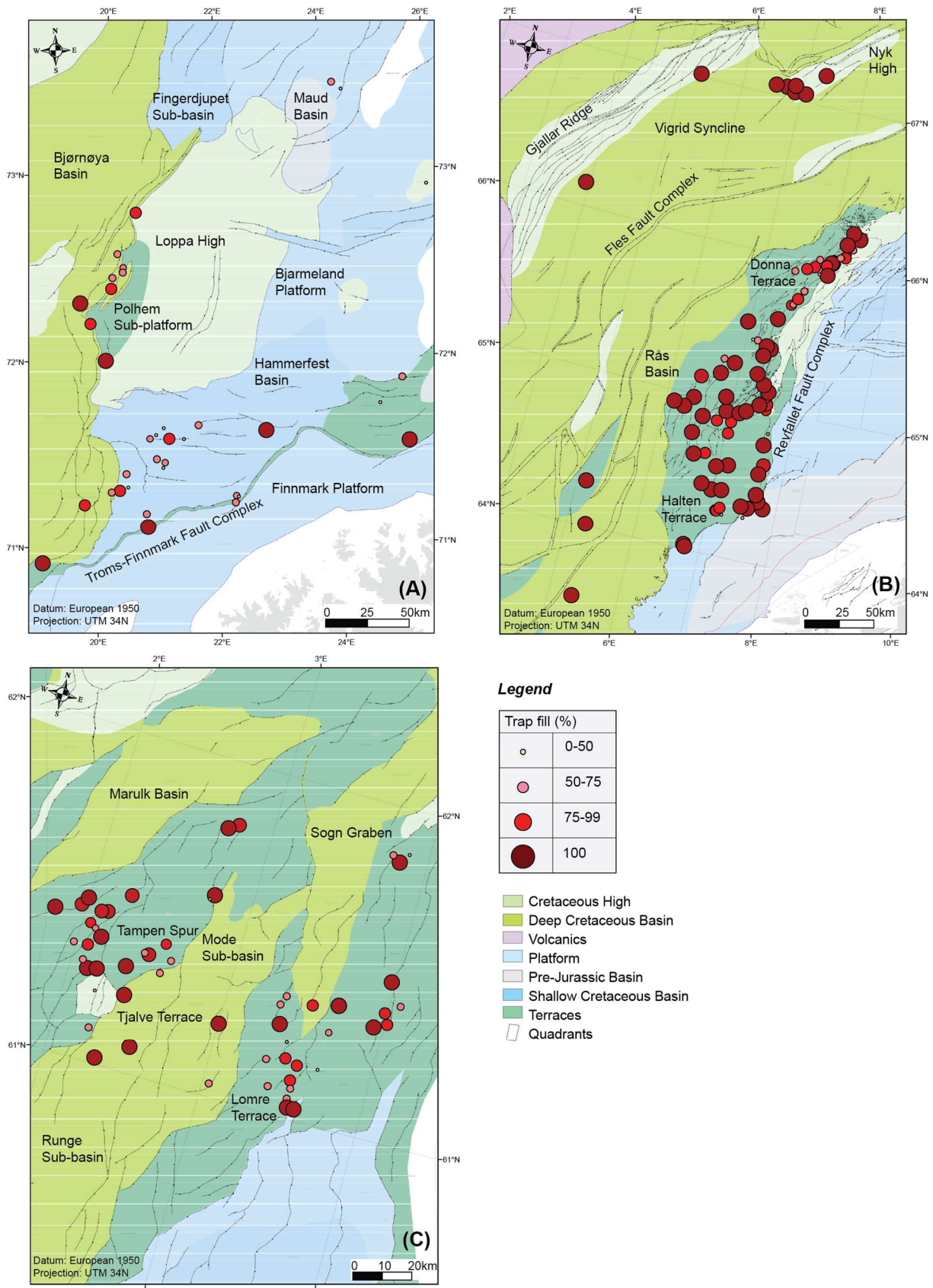
637

638

639

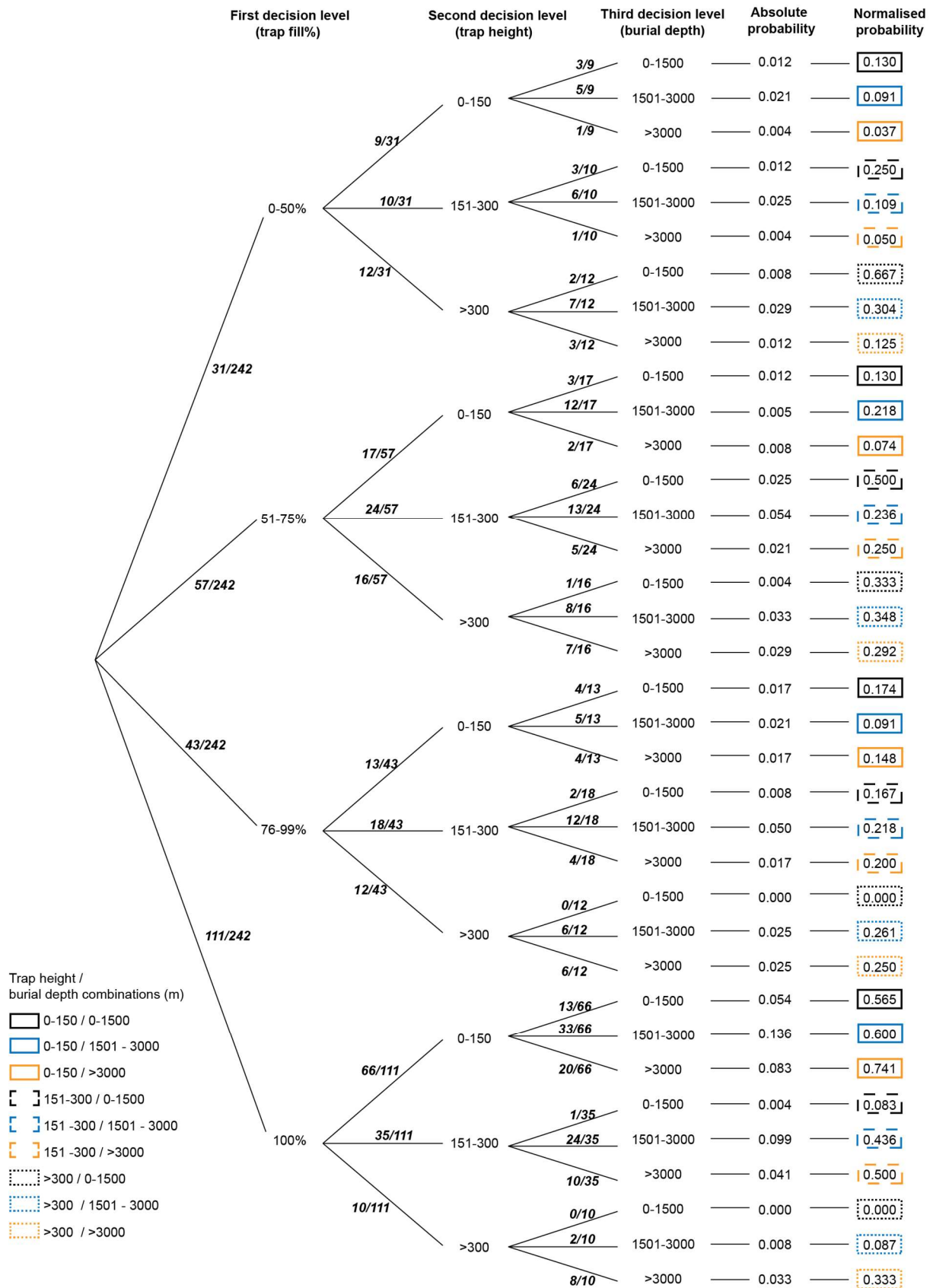
640

641 Figure 8

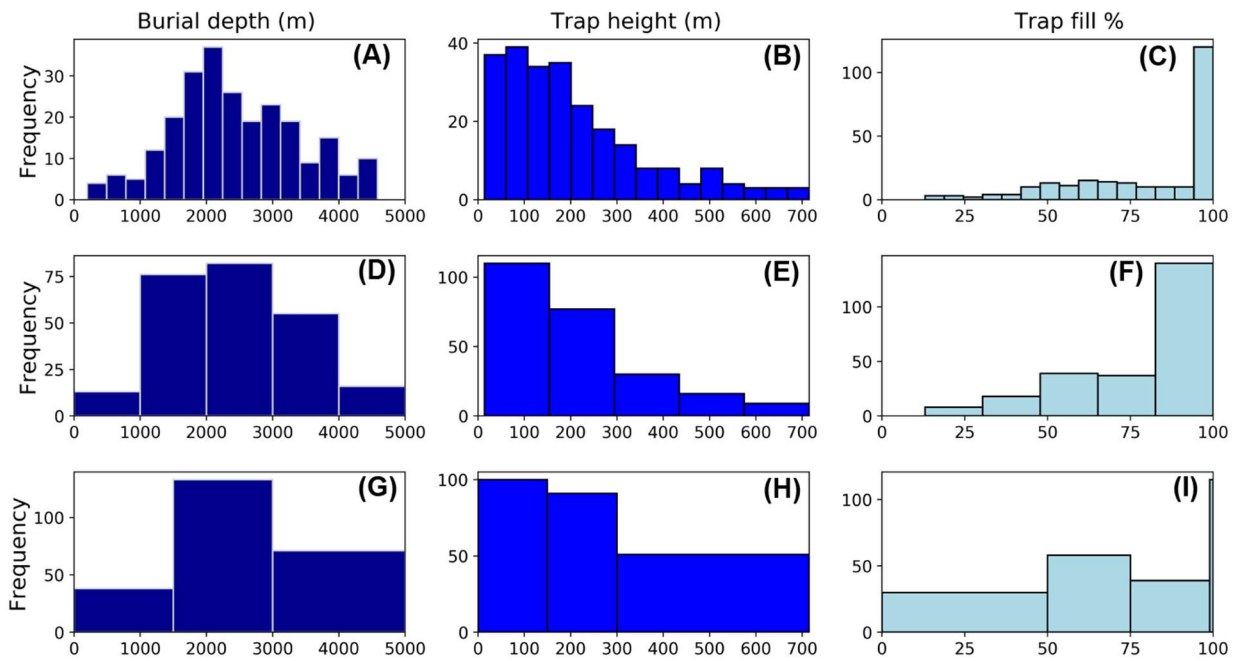


642

643 Figure 9

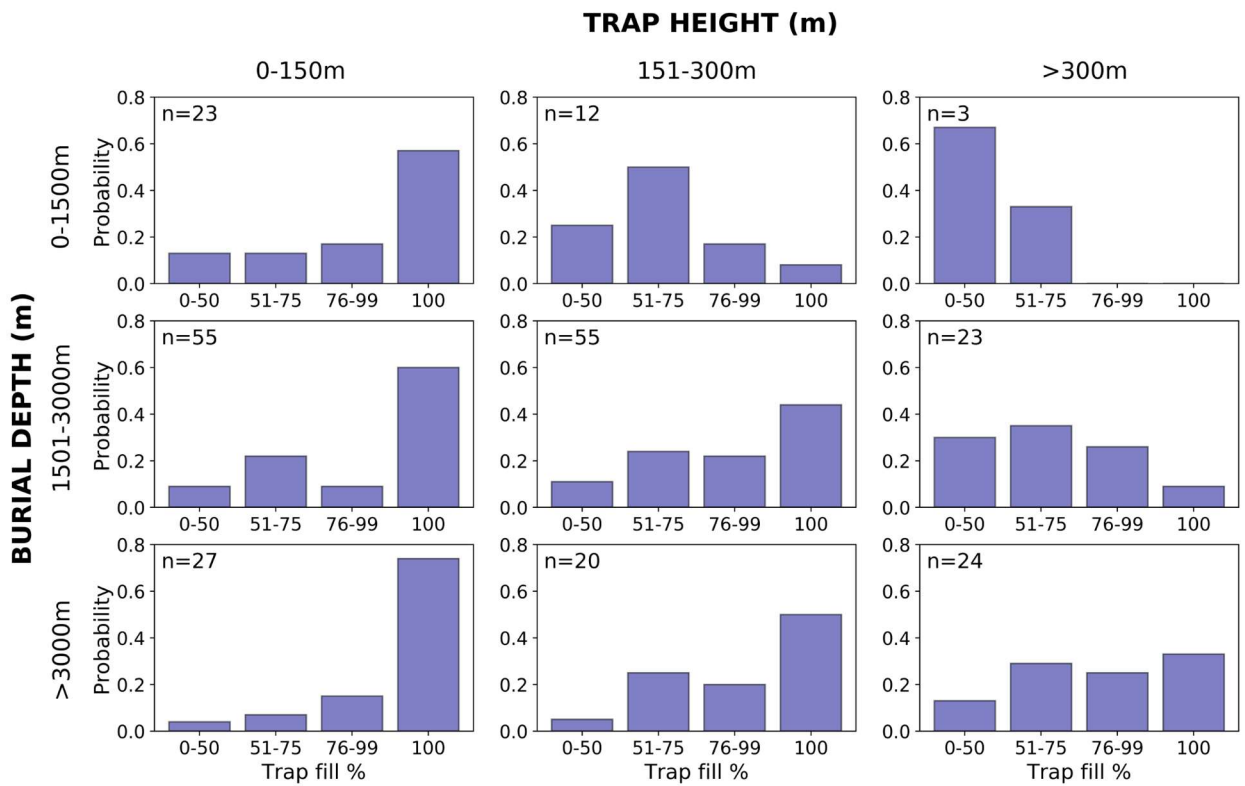


645 Figure 10



646

647 Figure 11



648

649 END